

DynamiCrafter: Animating Open-domain Images with Video Diffusion Priors

Jinbo Xing¹ Menghan Xia^{2,*} Yong Zhang² Haoxin Chen² Wangbo Yu³

Hanyuan Liu¹ Xintao Wang² Tien-Tsin Wong^{1,*} Ying Shan²

¹The Chinese University of Hong Kong ²Tencent AI Lab ³Peking University

Project page: <https://doubiu.github.io/projects/DynamiCrafter>

Abstract

Animating a still image offers an engaging visual experience. Traditional image animation techniques mainly focus on animating natural scenes with stochastic dynamics (e.g. clouds and fluid) or domain-specific motions (e.g. human hair or body motions), and thus limits their applicability to more general visual content. To overcome this limitation, we explore the synthesis of dynamic content for open-domain images, converting them into animated videos. The key idea is to utilize the motion prior of text-to-video diffusion models by incorporating the image into the generative process as guidance. Given an image, we first project it into a text-aligned rich context representation space using a query transformer, which facilitates the video model to digest the image content in a compatible fashion. However, some visual details still struggle to be preserved in the resultant videos. To supplement with more precise image information, we further feed the full image to the diffusion model by concatenating it with the initial noises. Experimental results show that our proposed method can produce visually convincing and more logical & natural motions, as well as higher conformity to the input image. Comparative evaluation demonstrates the notable superiority of our approach over existing competitors.

1. Introduction

Image animation has been a longstanding challenge in the fields of computer vision, with the goal of converting still images into video counterparts that display natural dynamics while preserving the original appearance of the images. Traditional heuristic approaches primarily concentrate on synthesizing stochastic and oscillating motions [40, 42] or customizing for specific object categories [31, 37]. However, the strong assumptions imposed on these methods limit their applicability in general scenarios, such as animating open-domain images. Recently, text-to-video (T2V)

generative models have achieved remarkable success in creating diverse and vivid videos from textual prompts. This inspires us to investigate the potential of leveraging such powerful video generation capabilities for image animation.

Our key idea is to govern the video generation process of T2V diffusion models by incorporating a conditional image. However, achieving the goal of image animation is still non-trivial, as it requires both visual context understanding (essential for creating dynamics) and detail preservation. Recent studies on multi-modal controllable video diffusion models, such as VideoComposer [77] and I2VGen-XL [12], have made preliminary attempts to enable video generation with visual guidance from an image. Unfortunately, both are incompetent for image animation due to their less comprehensive image injection mechanisms, which results in either abrupt temporal changes or low visual conformity to the input image (see Figure 4). To address this challenge, we propose a dual-stream image injection paradigm, comprised of text-aligned context representation and visual detail guidance, which ensures that the video diffusion model synthesizes detail-preserved dynamic content in a complementary manner. We call this approach *DynamiCrafter*.

Given an image, we first project it into the text-aligned rich context representation space through a specially designed context learning network. Specifically, it consists of a pre-trained CLIP image encoder to extract text-aligned image features and a learnable query transformer to further promote its adaptation to the diffusion models. The rich context features are used by the model via cross attention layers, which will then be combined with the text-conditioned features through gated fusion. In some extend, the learned context representation trades visual details with text alignment which helps facilitate semantic understanding of image context so that reasonable and vivid dynamics could be synthesized. To supplement more precise visual details, we further feed the full image to the diffusion model by concatenating it with the initial noise. This dual-stream injection paradigm guarantees both plausible dynamic content and visual conformity to the input image.

Extensive experiments are conducted to evaluate our

* Corresponding Authors.

proposed method, which demonstrates notable superiority over existing competitors and even comparable performance with the latest commercial demos (like Gen-2 [11] and PikaLabs [13]). Furthermore, we offer discussion and analysis on some insightful designs for diffusion model based image animation, such as the roles of different visual injection streams, the utility of text prompts and their potential for dynamics control, which may inspire follow-ups to push forward this line of technique. Besides of image animation, *DynamiCrafter* can be easily adapted to support applications like storytelling video generation, looping video generation, and generative frame interpolation. Our contributions are summarized as follows:

- We introduce an innovative approach for animating open-domain images by leveraging video diffusion prior, significantly outperforming contemporary competitors.
- We conduct a comprehensive analysis on the conditional space of text-to-video diffusion models and propose a dual-stream image injection paradigm to achieve the challenging goal of image animation.
- We pioneer the study of text-based motion control for open-domain image animation and demonstrate the proof of concept through preliminary experiments.

2. Related Work

2.1. Image Animation

Generating animation from still images is a heavily studied research area. Early physical simulation-based approaches [10, 36] focus on simulating the motion of specific objects, resulting in low generalizability due to the independent modeling of each object category. To produce more realistic motion, reference-based methods [9, 37, 51, 55, 63–65, 79] transfer motion or appearance information from reference signals, such as videos, to the synthesis process. Although they demonstrate better temporal coherence, the need for additional guidances limits their practical application. Additionally, a stream of works based on GAN [26, 38, 60] can generate frames by perturbing initial latents or performing random walk in the latent vector space. However, the generated motion is not plausible since the animated frames are just a visualization of the possible appearance space without temporal awareness. Recently, (learned) motion prior-based methods [16, 31, 34, 46, 49, 81, 82, 96] animate still images through explicit or implicit image-based rendering with estimated motion field or geometry priors. Similarly, video prediction [2, 18, 32, 33, 41, 74, 84, 86, 92] predicts future video frames starting from single images by learning spatio-temporal priors from video data.

Although existing approaches has achieved impressive performance, they primarily focus on animating motions in curated domains, particularly stochastic [5, 10, 14, 16, 36, 40, 51, 87] and oscillating [42] motion. Furthermore, the animated objects are limited to specific categories, *e.g.*,

fluid [31, 31, 45, 51], natural scenes [9, 36, 42, 60, 84], human hair [82], portraits [21, 78, 79], and bodies [4, 6, 37, 65, 79, 81]. In contrast, our work proposes a generic framework for animating open-domain images with a wide range of content and styles, which is extremely challenging due to the overwhelming complexity and vast diversity.

2.2. Video Diffusion Models

Diffusion models (DMs) [28, 67] have recently shown unprecedented generative power in text-to-image (T2I) generation [24, 50, 57–59, 95]. To replicate this success to video generation, the first video diffusion model (VDM) [30] is proposed to model low-resolution videos using a space-time factorized U-Net in pixel space. Imagen-Video [29] presents effective cascaded DMs with v-prediction for generating high-definition videos. To reduce training costs, subsequent studies [7, 23, 76, 80, 97] are engaged in transferring T2I to text-to-video (T2V) [20, 43, 66, 91], and learning VDMs in latent or hybrid-pixel-latent space.

Although these models can generate high-quality videos, they only accept text prompts as the sole semantic guidance, which can be vague and may not accurately reflect users' intention. Similar to adding controls in T2I [48, 61, 88, 93], introducing control signals in T2V, such as structure [17, 83], pose [44, 94], and Canny edge [39], has been increasingly receiving much attention. However, visual conditions in VDMs [71, 89], such as RGB images, remain under-explored. Most recently and concurrently, image condition is examined in Seer [22], VideoComposer [77], and I2VGen-XL [12] for (text-)image-to-video synthesis. However, they either focus on the curated domain, *i.e.*, indoor objects [22], or fail to generate temporally coherent frames and realistic motions [77] and preserve visual details of the input image [12] due to insufficient context understanding and loss of information of the input image. Moreover, recent proprietary T2V models [47, 66, 73, 90] have been demonstrated to be extensible to image-to-video synthesis. However, their results rarely adhere to the input image and suffers from the unrealistic temporal variation issue. Our approach is built upon text-conditioned VDMs to leverage their rich dynamic prior for animating open-domain images, by incorporating tailored designs for better semantic understanding and conformity to the input image.

3. Method

Given a still image, we aim at animating it to produce a short video clip, that inherits all the visual content from the image and exhibits an implicitly suggested and natural dynamics. Note that the still image can appear in the arbitrary location of the resultant frame sequence. Technically, such challenge can be formulated as a special kind of image-conditioned video generation that highly requires visual conformity. We tackle this synthesis task by utilizing the generative priors of pre-trained video diffusion models.

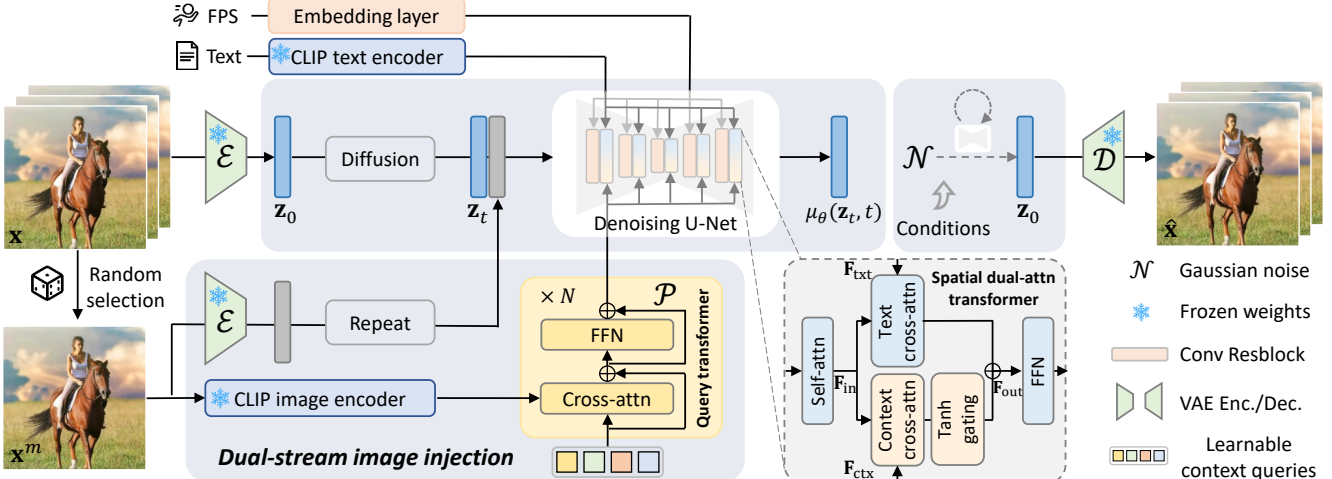


Figure 1. Flowchart of the proposed *DynamiCrafter*. During training, we randomly select a video frame as the image condition of the denoising process through the proposed dual-stream image injection mechanism to inherit visual details and digest the input image in a context-aware manner. During inference, our model can generate animation clips from noise conditioned on the input still image.

3.1. Preliminary: Video Diffusion Models

Diffusion models [28, 68] are generative models that define a forward diffusion process to convert data $\mathbf{x}_0 \sim p_{\text{data}}(\mathbf{x})$ into Gaussian noises $\mathbf{x}_T \sim \mathcal{N}(\mathbf{0}, \mathbf{I})$ and learn to reverse this process by denoising. The forward process $q(\mathbf{x}_t | \mathbf{x}_0, t)$ contains T timesteps, which gradually adds noise to the data sample \mathbf{x}_0 to yield \mathbf{x}_t through a parameterization trick. The denoising process $p_\theta(\mathbf{x}_{t-1} | \mathbf{x}_t, t)$ obtains less noisy data \mathbf{x}_{t-1} from the noisy input \mathbf{x}_t through a denoising network $\epsilon_\theta(\mathbf{x}_t, t)$, which is supervised by the objective:

$$\min_{\theta} \mathbb{E}_{t, \mathbf{x} \sim p_{\text{data}}, \epsilon \sim \mathcal{N}(\mathbf{0}, \mathbf{I})} \|\epsilon - \epsilon_\theta(\mathbf{x}_t, t)\|_2^2, \quad (1)$$

where ϵ is the sampled ground truth noise and θ indicates the learnable network parameters. Once the model is trained, we can obtain denoised data \mathbf{x}_0 from a random noise \mathbf{x}_T through iteratively denoising.

For video generation tasks, Latent Diffusion Models (LDMs) [29] are commonly used to reduce the computation complexity. In this paper, our study is conducted based on an open-source video LDM *VideoCrafter* [8]. Given a video $\mathbf{x} \in \mathbb{R}^{L \times 3 \times H \times W}$, we first encode it into a latent representation $\mathbf{z} = \mathcal{E}(\mathbf{x})$, $\mathbf{z} \in \mathbb{R}^{L \times C \times h \times w}$ frame-by-frame. Then, both the forward diffusion process $\mathbf{z}_t = p(\mathbf{z}_0, t)$ and backward denoising process $\mathbf{z}_t = p_\theta(\mathbf{z}_{t-1}, \mathbf{c}, t)$ are performed in this latent space, where \mathbf{c} denotes possible denoising conditions like text prompt. Accordingly, the generated videos are obtained through the decoder $\hat{\mathbf{x}} = \mathcal{D}(\mathbf{z})$.

3.2. Image Dynamics from Video Diffusion Priors

An open-domain text-to-video diffusion model is assumed to have diverse dynamic visual content modeled conditioning on text descriptions. To animate a still image with the T2V generative priors, the visual information should be injected into the video generation process in a comprehensive

manner. On the one hand, the image should be digested by the T2V model for context understanding, which is important for dynamics synthesis. On the other, the visual details should be preserved in the generated videos. Based on this insight, we propose a dual-stream conditional image injection paradigm, consisting of text-aligned context representation and visual detail guidance. The overview diagram is illustrated in Figure 1.

Text-aligned context representation. To guide video generation with image context, we propose to project the image into a text-aligned embedding space, so that the video model can utilize the image information in a compatible fashion. Since the text embedding is constructed with pre-trained CLIP [56] text encoder, we employ the image encoder counterpart to extract image feature from the input image. Although the global semantic token \mathbf{f}_{cls} from the CLIP image encoder is well-aligned with image captions, it mainly represents the visual content at the semantic level and fails to capture the image's full extent. To extract more complete information, we use the full visual tokens $\mathbf{F}_{\text{vis}} = \{\mathbf{f}_i^i\}_{i=1}^K$ from the last layer of the CLIP image ViT [15], which demonstrated high-fidelity in conditional image generation works [61, 88]. To promote the alignment with text embedding, in other words, to obtain a context representation that can be interpreted by the denoising U-Net, we utilize a learnable lightweight model \mathcal{P} to translate \mathbf{F}_{vis} into the final context representation $\mathbf{F}_{\text{ctx}} = \mathcal{P}(\mathbf{F}_{\text{vis}})$. We employ the query transformer architecture [1, 35] in multi-modal fusion studies as \mathcal{P} , which comprises N stacked layers of cross-attention and feed-forward networks (FFN), and is adept at cross-modal representation learning via the cross-attention mechanism.

Subsequently, the text embedding \mathbf{F}_{txt} and context embedding \mathbf{F}_{ctx} are employed to interact with the U-Net inter-

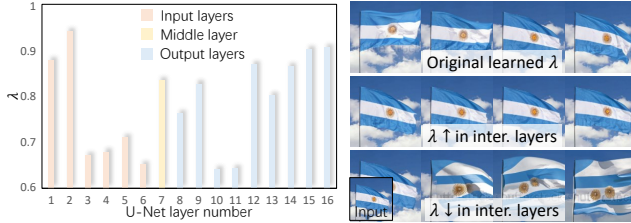


Figure 2. Visualization of the learned λ across U-Net layers (left), and visual comparisons when manually adjusting λ (right).

mediate features \mathbf{F}_{in} through the dual cross-attention layers:

$$\mathbf{F}_{\text{out}} = \text{Softmax}\left(\frac{\mathbf{Q}\mathbf{K}_{\text{txt}}^{\top}}{\sqrt{d}}\right)\mathbf{V}_{\text{txt}} + \lambda \cdot \text{Softmax}\left(\frac{\mathbf{Q}\mathbf{K}_{\text{ctx}}^{\top}}{\sqrt{d}}\right)\mathbf{V}_{\text{ctx}}, \quad (2)$$

where $\mathbf{Q} = \mathbf{F}_{\text{in}}\mathbf{W}_Q$, $\mathbf{K}_{\text{txt}} = \mathbf{F}_{\text{txt}}\mathbf{W}_K$, $\mathbf{V}_{\text{txt}} = \mathbf{F}_{\text{txt}}\mathbf{W}_V$, and $\mathbf{K}_{\text{ctx}} = \mathbf{F}_{\text{ctx}}\mathbf{W}'_K$, $\mathbf{V}_{\text{ctx}} = \mathbf{F}_{\text{ctx}}\mathbf{W}'_V$ accordingly. In particular, λ denotes the coefficient that fuses text-conditioned and image-conditioned features, which is achieved through \tanh gating and adaptively learnable for each layers. This design aims to facilitate the model’s ability to absorb image conditions in a layer-dependent manner. As the intermediate layers of the U-Net are more associated with object shapes or poses, and the two-end layers are more linked to appearance [75], we expect that the image features will primarily influence the videos’ appearance while exerting relatively less impact on the shape.

Observations and analysis of λ . Figure 2 (left) illustrates the learned coefficients across different layers, indicating that the image information has a more significant impact on the two-end layers w.r.t. the intermediate layers. To explore further, we manually alter λ in the intermediate layers. As depicted in Figure 2 (right), increasing λ leads to suppressed cross-frame movements, while decreasing λ poses challenges in preserving the object’s shape. This observation not only align with our expectations, but also suggests that in image-conditioned diffusion models, rich-context information influences certain intermediate layers (*e.g.*, layers 7-9) of the U-Net, enabling the model to maintain object shape similar to the input in the presence of motions.

Visual detail guidance (VDG). The rich-informative context representation enables the video diffusion model to produce videos that closely resemble the input image. However, as shown in Figure 3, minor discrepancies may still occur. This is mainly due to the pre-trained CLIP image encoder’s limited capability to fully preserve input image information, as it is designed to align visual and language features. To enhance visual conformity, we propose providing the video model with additional visual details from the image. Specifically, we concatenate the conditional image with per-frame initial noise and feed them to the denoising U-Net as a form of guidance. Therefore, in our proposed dual-stream image injection paradigm, the video diffusion



Figure 3. (Left) Comparison of animations produced using rich context representation solely, and additionally visual detail guidance (VDG). (Right) Impact of text with context representation.

model integrates both global context and local details from the input image in a complementary fashion.

Discussion. (i) *Why are text prompts necessary when a more informative context representation is provided?* Although we construct a text-aligned context representation, it carries more extensive information than text embedding, which may overburden the T2V model to digest them properly, *e.g.*, causing shape distortion. Additional text prompts can offer a native global context that enables the model to efficiently utilize image information. Figure 3 (right) demonstrates how incorporating text can address the issue of shape distortion in the bear’s head. Furthermore, as a still image typically contains multiple potential dynamic variations, text prompts can effectively guide the generation of dynamic content tailored to user preferences (see Sec. 5). (ii) *Why is a rich context representation necessary when the visual guidance provides the complete image?* As previously mentioned, the pre-trained T2V model comprises a semantic control space (text embedding) and a complementary random space (initial noise). While the random space effectively integrates low-level information, concatenating the noise of each frame with a fixed image induces spatial misalignment potentially, which may misguide the model in uncontrollable directions. Regarding this, the precise visual context supplied by the image embedding can assist in the reliable utilization of visual details. The corresponding ablation study is presented in Sec. 4.4.

3.3. Training Paradigm

The conditional image is integrated through two complementary streams, which play roles in context control and detail guidance, respectively. To modulate them in a cooperative manner, we device a dedicated training strategy consisting of three stages, *i.e.*, (i) training the image context representation network \mathcal{P} , (ii) adapting \mathcal{P} to the T2V model, and (iii) joint fine-tuning with VDG.

Specifically, to offer the image information to the T2V model in a compatible fashion, we propose to train a context representation network \mathcal{P} to extract text-aligned visual information from the input image. Considering the fact that \mathcal{P} takes numerous optimization steps to converge, we propose to train it based on a lightweight T2I model instead of

a T2V model, allowing it to focus on image context learning, and then adapt it to the T2V model by jointly training \mathcal{P} and spatial layers (in contrast to temporal layers) of the T2V model. After establishing a compatible context conditioning branch for T2V, we concatenate the input image with per-frame noise for joint fine-tuning to enhance visual conformity. Here we only fine-tune \mathcal{P} and the VDM’s spatial layers to avoid disrupting the pre-trained T2V model’s temporal prior knowledge with dense image concatenation, which could lead to significant performance degradation and contradict our original intention. Additionally, we randomly select a video frame as the image condition based on two considerations: (i) to prevent the network from learning a shortcut that maps the concatenated image to a frame in the specific location, and (ii) to force the context representation to be more flexible to avoid offering the over-rigid information for a specific frame, *i.e.*, the objective in the context learning based on T2I.

4. Experiment

4.1. Implementation Details

Our development is based on the open-source T2V model VideoCrafter [8] (@ 256×256 resolution) and T2I model Stable-Diffusion-v2.1 (SD) [58]. We firstly train \mathcal{P} and the newly injected image cross-attention layers based on SD, with 1000K steps on the learning rate 1×10^{-4} and valid mini-batch size 64. Then we replace SD with VideoCrafter and further fine-tune \mathcal{P} and spatial layers with 30K steps for adaptation, and additional 100K steps with image concatenation on the learning rate 5×10^{-5} and valid mini-batch size 64. Our DynamiCrafter was trained on WebVid-10M [3] dataset by sampling 16 frames with dynamic FPS at the resolution of 256×256 in a batch. At inference, we adopt DDIM sampler [69] with multi-condition classifier-free guidance [27]. Specifically, similar to video editing [17], we introduce two guidance scales s_{img} and s_{txt} to text-conditioned image animation, which can be adjusted to trade off the impact of two control signals:

$$\begin{aligned} \hat{\epsilon}_{\theta}(\mathbf{z}_t, \mathbf{c}_{\text{img}}, \mathbf{c}_{\text{txt}}) &= \epsilon_{\theta}(\mathbf{z}_t, \emptyset, \emptyset) \\ &\quad + s_{\text{img}}(\epsilon_{\theta}(\mathbf{z}_t, \mathbf{c}_{\text{img}}, \emptyset) - \epsilon_{\theta}(\mathbf{z}_t, \emptyset, \emptyset)) \\ &\quad + s_{\text{txt}}(\epsilon_{\theta}(\mathbf{z}_t, \mathbf{c}_{\text{img}}, \mathbf{c}_{\text{txt}}) - \epsilon_{\theta}(\mathbf{z}_t, \mathbf{c}_{\text{img}}, \emptyset)). \end{aligned}$$

4.2. Quantitative Evaluation

Metrics and datasets. To evaluate the quality and temporal coherence of synthesized videos in both the spatial and temporal domains, we report Fréchet Video Distance (FVD) [72] as well as Kernel Video Distance (KVD) [72]. Following [7, 97], we evaluate the zero-shot generation performance of all the methods on UCF-101 [70] and MSR-VTT [85]. To further investigate the perceptual conformity between the input image and the animation results, we introduce Perceptual Input Conformity (PIC), which is com-

Table 1. Quantitative comparisons with state-of-the-art open-domain image-to-video generation methods on UCF-101 and MSR-VTT for the zero-shot setting.

Method	UCF-101			MSR-VTT		
	FVD ↓	KVD ↓	PIC ↑	FVD ↓	KVD ↓	PIC ↑
VideoComposer	576.81	65.56	0.5269	377.29	26.34	0.4460
I2VGen-XL	571.11	58.59	0.5313	289.10	14.70	0.5352
Ours	429.23	62.47	0.6078	234.66	13.74	0.5803

puted by $\frac{1}{L} \sum_l (1 - D(\mathbf{x}^{\text{in}}, \mathbf{x}^l))$, where $\mathbf{x}^{\text{in}}, \mathbf{x}^l, L$ are the input image, video frames, and video length, respectively, and we adopt the perceptual distance metric DreamSim [19] as the distance function $D(\cdot, \cdot)$. We evaluate each error metric at the resolution of 256×256 with 16 frames.

As open-domain image animation is a nascent area of computer vision, there are limited publicly available research works for comparison. We evaluate our method against VideoComposer [77] and I2VGen-XL [12], with the quantitative results presented in Table 1. According to the results, our proposed method significantly outperforms previous approaches in all evaluation metrics, except for KVD on UCF-101, thanks to the effective dual-stream image injection design for fully exploiting the video diffusion prior.

4.3. Qualitative Evaluation

In addition to the aforementioned approaches, we include two more proprietary commercial products, *i.e.*, PikaLabs [13] and Gen-2 [11], for qualitative comparison. Note that the results we accessed on Nov. 1st, 2023 might differ from the current product version due to rapid version iterations. Figure 4 presents the visual comparison of image animation results with various content and styles. Among all compared methods, our approach generates temporally coherent videos that adhere to the input image condition. In contrast, VideoComposer struggles to produce consistent video frames, as subsequent frames tend to deviate from the initial frame due to inadequate semantic understanding of the input image. I2VGen-XL can generate videos that semantically resemble the input images but fails to preserve intricate local visual details and produce aesthetically appealing results. As commercial products, PikaLabs and Gen-2 can produce appealing high-resolution and long-duration videos. However, Gen-2 suffers from sudden content changes (the ‘Windmill’ case) and content drifting issues (‘The Beatles’ and ‘Girl’ cases). PikaLabs tends to generate still videos with less dynamic and exhibits blurriness when attempting to produce larger dynamics (‘The Beatles’ case). It is worth noting that our method allows dynamic control through text prompts while other methods suffers from neglecting the text modality (*e.g.*, *talking* in the ‘Girl’ case). More videos are provided in the *Supplement*.

User study. We conduct a user study to evaluate the perceptual quality of the generated images. The participants



Figure 4. Visual comparisons of image animation results from VideoComposer, I2VGen-XL, PikaLabs, Gen-2, and our DynamiCrafter.

Table 2. User study statistics of the preference rate for Motion Quality (M.Q.) & Temporal Coherence (T.C.), and selection rate for visual conformity to the input image (I.C.=Input Conformity).

Property	Proprietary		Open-source		
	PikaLabs	Gen-2	VideoComposer	I2VGen-XL	Ours
M.Q. ↑	28.60%	22.91%	2.09%	7.56%	38.84%
T.C. ↑	32.09%	26.05%	2.21%	6.51%	33.14%
I.C. ↑	79.07%	64.77%	18.14%	15.00%	79.88%

are asked to choose the best result in terms of motion quality and temporal coherence, and to select the results

with good visual conformity to the input image for each case. The statistics from 49 participants’ responses are presented in Table 2. Our method demonstrates significant superiority over other open-source methods. Moreover, our method achieves comparable performance in terms of temporal coherence and input conformity compared to commercial products, while exhibiting superior motion quality.

4.4. Ablation Studies

Dual-stream image injection. To investigate the roles of each image conditioning stream, we examine two variants:

Table 3. Ablation study on the dual-stream image injection and training paradigm.

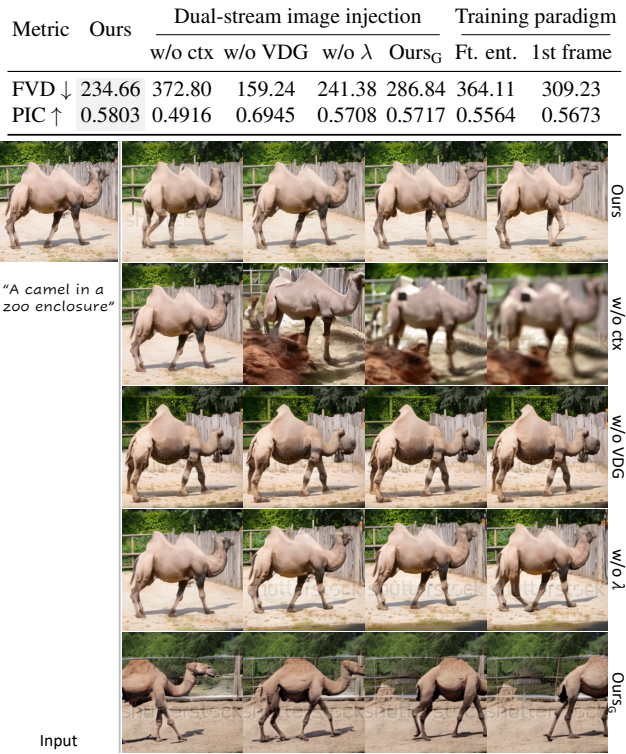


Figure 5. Visual comparisons of different variants of our method.

i). **Ours w/o ctx**, by removing the context conditioning stream, ii). **Ours w/o VDG**, by removing the visual detail guidance stream. Table 3 presents a quantitative comparison between our full method and these variants. The performance of ‘w/o ctx’ declines significantly due to its inability to semantically comprehend the input image without injection of rich-context representation, leading to temporal inconsistencies in the generated videos (see the 2nd row in Figure 5). Although removing the VDG (w/o VDG) can yield better FVD scores, it causes severe shape distortions and exhibits limited motion magnitude, as the remaining context condition can only provide semantic-level image information. Moreover, while it achieves a higher PIC score, it fails to capture all the visual details of the input image, as evidenced by the 3rd row in Figure 5.

We then study several key designs in the context representation stream: adaptive gating λ and full visual tokens in CLIP image encoder. Eliminating the adaptive gating λ (w/o λ) leads to a slight decrease in model performance. This is because, without considering the nature of the denoising U-Net layers, context information cannot be adaptively integrated into the T2V model, resulting in shaky generated videos and unnatural motions (see the 4th row in Figure 5). On the other hand, using a strategy (Ours_G) like I2VGen-XL that utilizes a single CLIP global token may generate results that are only semantically similar to the in-



Figure 6. Visual comparisons of the context conditioning stream learned in one-stage and our two-stage adaption strategy.



Figure 7. Visual comparisons of different training paradigms.

put due to the absence of full image extent. In contrast, our full method effectively leverages the video diffusion prior for image animation with natural motion, coherent frames, and visual conformity to the input image.

Training paradigm. We further examine the specialized training paradigm to ensure the model works as expectation. We firstly construct a baseline by training the context representation network \mathcal{P} based on the pre-trained T2V and keeping other settings unchanged. As illustrated in Figure 6, this baseline (one-stage) converges at a significantly slow pace, resulting in only coarse-grained context conditioning with the same optimization steps. This may potentially make it challenging for the T2V model to harmonize the dual-stream conditions after incorporating the VDG.

After obtaining a compatible context conditioning stream \mathcal{P} , we further incorporate image concatenation with per-frame noise to enhance visual conformity by jointly fine-tuning \mathcal{P} and *spatial layers* of the T2V model. We construct a baseline by fine-tuning the entire T2V model, and the quantitative comparison in Table 3 (Ft. ent.) shows that this baseline results in an unstable model that is prone to collapse, disrupting the temporal prior. Additionally, to study the effectiveness of our random selection conditioning strategy, we train a baseline (1st frame cond.) that consistently uses the first video frame as the conditional image. Table 3 reveals its inferior performance in terms of both FVD and PIC, which can be attributed to the “content sudden change” effect observed in the generated videos (Figure 7 (bottom)). We hypothesize that the model may dis-

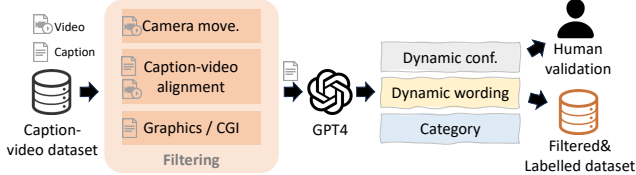


Figure 8. Illustration of dataset filtering and annotation process.



Figure 9. Visual comparisons of image animation results from different methods with motion control using text.

cover a suboptimal shortcut for mapping the concatenated image to the first frame while neglecting other frames.

5. Discussions on Motion Control using Text

Since images are typically associated with multiple potential dynamics in its context, text can complementarily guide the generation of dynamic content tailored to user preference. However, captions in existing large-scale datasets often consist of a combination of a large number of scene descriptive words and less dynamic/motion descriptions, potentially causing the model to overlook dynamics/motions during learning. For image animation, the scene description is already included in the image condition, while the motion description should be treated as text condition to train the model in a *decoupled* manner, providing the model with stronger text-based control over dynamics.

Dataset construction. To enable the decoupled training, we construct a dataset by filtering and re-annotating the WebVid10M dataset, as illustrated in Figure 8. The constructed dataset contains captions with purer *dynamic wording*, such as “Man doing push-ups.”, and categories, *e.g.*, human.

We then train a model DynamiCrater_{DCP} using the dataset and validate its effectiveness with 40 image-prompt testing cases featuring human figures with ambiguous potential actions, and prompts describing various motions



Figure 10. Applications of our *DynamiCrafter*. □: input images.

(*e.g.*, “Man waving hands” and “Man clapping”). We measure the average CLIP similarity (CLIP-SIM) between the prompt and video results, and DynamiCrater_{DCP} improves the performance from 0.17 to 0.19 in terms of CLIP-SIM score. The visual comparison in Figure 9 shows that Gen-2 and PikaLabs cannot support motion control using text, while our DynamiCrafter reflects the text prompt and is further enhanced in DynamiCrafter_{DCP} with the proposed de-coupled training. More details are in the *Supplement*.

6. Applications

DynamiCrafter can be easily adapted to support additional applications. **i). Storytelling with shots.** First, we utilize ChatGPT (equipped with DALL-E 3 [62]) to generate a story script and corresponding shots (images). And then storytelling videos can be generated by animating those shots with story scripts using DynamiCrafter, as displayed in Figure 10 (top). **ii). Looping video generation.** With minor modifications, our framework can be adapted to facilitate the generation of looping videos. Specifically, we provide both x^1 and x^L as visual detail guidance and leave other frames as empty during training. During inference, we set both of them as the input image. Additionally, we experiment with building this application on top of a higher-resolution (320×512) version of VideoCrafter. The looping video result is shown in Figure 10 (middle). **iii). Generative frame interpolation.** Furthermore, the modified model enables generative frame interpolation by set the input images x^1 and x^L differently, as shown in Figure 10 (bottom).

7. Conclusion

In this study, we introduced *DynamiCrafter*, an effective framework for animating open-domain images by leveraging pre-trained video diffusion priors with the proposed dual-stream image injection mechanism and dedicated training paradigm. Our experimental results highlight the effectiveness and superiority of our approach compared to existing methods. Furthermore, we explored text-based dynamic control for image animation with the constructed dataset. Lastly, we demonstrated the versatility of our framework across various applications and scenarios.

References

- [1] Anas Awadalla, Irena Gao, Josh Gardner, Jack Hessel, Yusuf Hanafy, Wanrong Zhu, Kalyani Marathe, Yonatan Bitton, Samir Gadre, Shiori Sagawa, et al. Openflamingo: An open-source framework for training large autoregressive vision-language models. *arXiv preprint arXiv:2308.01390*, 2023. 3
- [2] Mohammad Babaeizadeh, Chelsea Finn, Dumitru Erhan, Roy Campbell, and Sergey Levine. Stochastic variational video prediction. In *ICLR*, 2018. 2
- [3] Max Bain, Arsha Nagrani, GüL Varol, and Andrew Zisserman. Frozen in time: A joint video and image encoder for end-to-end retrieval. In *ICCV*, 2021. 5
- [4] Hugo Bertiche, Niloy J Mitra, Kuldeep Kulkarni, Chun-Hao P Huang, Tuanfeng Y Wang, Meysam Madadi, Sergio Escalera, and Duygu Ceylan. Blowing in the wind: Cyclenet for human cinemagraphs from still images. In *CVPR*, 2023. 2
- [5] Andreas Blattmann, Timo Milbich, Michael Dorkenwald, and Björn Ommer. ipoke: Poking a still image for controlled stochastic video synthesis. In *ICCV*, 2021. 2
- [6] Andreas Blattmann, Timo Milbich, Michael Dorkenwald, and Björn Ommer. Understanding object dynamics for interactive image-to-video synthesis. In *CVPR*, 2021. 2
- [7] Andreas Blattmann, Robin Rombach, Huan Ling, Tim Dockhorn, Seung Wook Kim, Sanja Fidler, and Karsten Kreis. Align your latents: High-resolution video synthesis with latent diffusion models. In *CVPR*, 2023. 2, 5, 12, 13
- [8] Haoxin Chen, Menghan Xia, Yingqing He, Yong Zhang, Xiaodong Cun, Shaoshu Yang, Jinbo Xing, Yaofang Liu, Qifeng Chen, Xintao Wang, et al. Videocrafter1: Open diffusion models for high-quality video generation. *arXiv preprint arXiv:2310.19512*, 2023. 3, 5, 12
- [9] Chia-Chi Cheng, Hung-Yu Chen, and Wei-Chen Chiu. Time flies: Animating a still image with time-lapse video as reference. In *CVPR*, 2020. 2
- [10] Yung-Yu Chuang, Dan B Goldman, Ke Colin Zheng, Brian Curless, David H Salesin, and Richard Szeliski. Animating pictures with stochastic motion textures. In *ACM SIGGRAPH*, 2005. 2
- [11] Gen-2 contributors. Gen-2. *Gen-2*. Accessed Nov. 1, 2023 [Online] <https://research.runwayml.com/gen2/>. 2, 5, 13
- [12] I2VGen-XL contributors. I2vgen-xl. Accessed October 15, 2023 [Online] <https://modelscope.cn/models/damo/Image-to-Video/summary/>. 1, 2, 5, 13
- [13] PikaLabs contributors. Pikalabs. *PikaLabs*. Accessed Nov. 1, 2023 [Online] <https://www.pika.art/>. 2, 5, 13
- [14] Michael Dorkenwald, Timo Milbich, Andreas Blattmann, Robin Rombach, Konstantinos G Derpanis, and Björn Ommer. Stochastic image-to-video synthesis using cinns. In *CVPR*, 2021. 2
- [15] Alexey Dosovitskiy, Lucas Beyer, Alexander Kolesnikov, Dirk Weissenborn, Xiaohua Zhai, Thomas Unterthiner, Mostafa Dehghani, Matthias Minderer, Georg Heigold, Sylvain Gelly, et al. An image is worth 16x16 words: Transformers for image recognition at scale. In *ICLR*, 2020. 3
- [16] Yuki Endo, Yoshihiro Kanamori, and Shigeru Kuriyama. Animating landscape: self-supervised learning of decoupled motion and appearance for single-image video synthesis. *ACM TOG*, 38(6):1–19, 2019. 2
- [17] Patrick Esser, Johnathan Chiu, Parmida Atighetchian, Jonathan Granskog, and Anastasis Germanidis. Structure and content-guided video synthesis with diffusion models. In *ICCV*, 2023. 2, 5
- [18] Jean-Yves Franceschi, Edouard Delasalles, Mickaël Chen, Sylvain Lamprier, and Patrick Gallinari. Stochastic latent residual video prediction. In *ICML*, 2020. 2
- [19] Stephanie Fu, Netanel Tamir, Shobhita Sundaram, Lucy Chai, Richard Zhang, Tali Dekel, and Phillip Isola. Dreamsim: Learning new dimensions of human visual similarity using synthetic data. In *NeurIPS*, 2023. 5
- [20] Songwei Ge, Seungjun Nah, Guilin Liu, Tyler Poon, Andrew Tao, Bryan Catanzaro, David Jacobs, Jia-Bin Huang, Ming-Yu Liu, and Yogesh Balaji. Preserve your own correlation: A noise prior for video diffusion models. In *ICCV*, 2023. 2
- [21] Jiahao Geng, Tianjia Shao, Youyi Zheng, Yanlin Weng, and Kun Zhou. Warp-guided gans for single-photo facial animation. *ACM TOG*, 37(6):1–12, 2018. 2
- [22] Xianfan Gu, Chuan Wen, Jiaming Song, and Yang Gao. Seer: Language instructed video prediction with latent diffusion models. *arXiv preprint arXiv:2303.14897*, 2023. 2
- [23] Yingqing He, Tianyu Yang, Yong Zhang, Ying Shan, and Qifeng Chen. Latent video diffusion models for high-fidelity video generation with arbitrary lengths. *arXiv preprint arXiv:2211.13221*, 2022. 2
- [24] Yingqing He, Shaoshu Yang, Haoxin Chen, Xiaodong Cun, Menghan Xia, Yong Zhang, Xintao Wang, Ran He, Qifeng Chen, and Ying Shan. Scalecrafter: Tuning-free higher-resolution visual generation with diffusion models. *arXiv preprint arXiv:2310.07702*, 2023. 2
- [25] Dan Hendrycks and Kevin Gimpel. Gaussian error linear units (gelus). *arXiv preprint arXiv:1606.08415*, 2016. 12
- [26] Tobias Hinz, Matthew Fisher, Oliver Wang, and Stefan Wermter. Improved techniques for training single-image gans. In *WACV*, 2021. 2
- [27] Jonathan Ho and Tim Salimans. Classifier-free diffusion guidance. *arXiv preprint arXiv:2207.12598*, 2022. 5, 15
- [28] Jonathan Ho, Ajay Jain, and Pieter Abbeel. Denoising diffusion probabilistic models. In *NeurIPS*, 2020. 2, 3
- [29] Jonathan Ho, William Chan, Chitwan Saharia, Jay Whang, Ruiqi Gao, Alexey Gritsenko, Diederik P Kingma, Ben Poole, Mohammad Norouzi, David J Fleet, et al. Imagen video: High definition video generation with diffusion models. *arXiv preprint arXiv:2210.02303*, 2022. 2, 3
- [30] Jonathan Ho, Tim Salimans, Alexey Gritsenko, William Chan, Mohammad Norouzi, and David J Fleet. Video diffusion models. In *NeurIPS*, 2022. 2
- [31] Aleksander Holynski, Brian L Curless, Steven M Seitz, and Richard Szeliski. Animating pictures with eulerian motion fields. In *CVPR*, 2021. 1, 2
- [32] Tobias Höppe, Arash Mehrjou, Stefan Bauer, Didrik Nielsen, and Andrea Dittadi. Diffusion models for video prediction and infilling. *TMLR*, 2022. 2

- [33] Xiaotao Hu, Zhewei Huang, Ailin Huang, Jun Xu, and Shuchang Zhou. A dynamic multi-scale voxel flow network for video prediction. In *CVPR*, 2023. 2
- [34] Yaosi Hu, Chong Luo, and Zhenzhong Chen. Make it move: controllable image-to-video generation with text descriptions. In *CVPR*, 2022. 2
- [35] Andrew Jaegle, Felix Gimeno, Andy Brock, Oriol Vinyals, Andrew Zisserman, and Joao Carreira. Perceiver: General perception with iterative attention. In *ICML*, 2021. 3
- [36] Wei-Cih Jhou and Wen-Huang Cheng. Animating still landscape photographs through cloud motion creation. *IEEE TMM*, 18(1):4–13, 2015. 2
- [37] Johanna Karras, Aleksander Holynski, Ting-Chun Wang, and Ira Kemelmacher-Shlizerman. Dreampose: Fashion image-to-video synthesis via stable diffusion. *arXiv preprint arXiv:2304.06025*, 2023. 1, 2
- [38] Tero Karras, Samuli Laine, Miika Aittala, Janne Hellsten, Jaakko Lehtinen, and Timo Aila. Analyzing and improving the image quality of stylegan. In *CVPR*, 2020. 2
- [39] Levon Khachatryan, Andranik Moysisyan, Vahram Tadevosyan, Roberto Henschel, Zhangyang Wang, Shant Navasardyan, and Humphrey Shi. Text2video-zero: Text-to-image diffusion models are zero-shot video generators. *arXiv preprint arXiv:2303.13439*, 2023. 2
- [40] Alex X Lee, Richard Zhang, Frederik Ebert, Pieter Abbeel, Chelsea Finn, and Sergey Levine. Stochastic adversarial video prediction. *arXiv preprint arXiv:1804.01523*, 2018. 1, 2
- [41] Yijun Li, Chen Fang, Jimei Yang, Zhaowen Wang, Xin Lu, and Ming-Hsuan Yang. Flow-grounded spatial-temporal video prediction from still images. In *ECCV*, 2018. 2
- [42] Zhengqi Li, Richard Tucker, Noah Snavely, and Aleksander Holynski. Generative image dynamics. *arXiv preprint arXiv:2309.07906*, 2023. 1, 2
- [43] Zhengxiong Luo, Dayou Chen, Yingya Zhang, Yan Huang, Liang Wang, Yujun Shen, Deli Zhao, Jingren Zhou, and Tieniu Tan. Videofusion: Decomposed diffusion models for high-quality video generation. In *CVPR*, 2023. 2
- [44] Yue Ma, Yingqing He, Xiaodong Cun, Xintao Wang, Ying Shan, Xiu Li, and Qifeng Chen. Follow your pose: Pose-guided text-to-video generation using pose-free videos. *arXiv preprint arXiv:2304.01186*, 2023. 2
- [45] Aniruddha Mahapatra and Kuldeep Kulkarni. Controllable animation of fluid elements in still images. In *CVPR*, 2022. 2
- [46] Arun Mallya, Ting-Chun Wang, and Ming-Yu Liu. Implicit warping for animation with image sets. In *NeurIPS*, 2022. 2
- [47] Eyal Molad, Eliah Horwitz, Dani Valevski, Alex Rav Acha, Yossi Matias, Yael Pritch, Yaniv Leviathan, and Yedid Hoshen. Dreamix: Video diffusion models are general video editors. *arXiv preprint arXiv:2302.01329*, 2023. 2
- [48] Chong Mou, Xintao Wang, Liangbin Xie, Jian Zhang, Zhonggang Qi, Ying Shan, and Xiaohu Qie. T2i-adapter: Learning adapters to dig out more controllable ability for text-to-image diffusion models. *arXiv preprint arXiv:2302.08453*, 2023. 2
- [49] Haomiao Ni, Changhao Shi, Kai Li, Sharon X Huang, and Martin Renqiang Min. Conditional image-to-video generation with latent flow diffusion models. In *CVPR*, 2023. 2
- [50] Alexander Quinn Nichol, Prafulla Dhariwal, Aditya Ramesh, Pranav Shyam, Pamela Mishkin, Bob McGrew, Ilya Sutskever, and Mark Chen. Glide: Towards photorealistic image generation and editing with text-guided diffusion models. In *ICML*, 2022. 2
- [51] Makoto Okabe, Ken Anjyo, Takeo Igarashi, and Hans-Peter Seidel. Animating pictures of fluid using video examples. In *CGF*, pages 677–686, 2009. 2
- [52] OpenAI. Gpt-4 technical report, 2023. 13
- [53] Junting Pan, Keqiang Sun, Yuying Ge, Hao Li, Haodong Duan, Xiaoshi Wu, Renrui Zhang, Aojun Zhou, Zipeng Qin, Yi Wang, et al. Journeydb: A benchmark for generative image understanding. *arXiv preprint arXiv:2307.00716*, 2023. 20
- [54] Jordi Pont-Tuset, Federico Perazzi, Sergi Caelles, Pablo Arbelaez, Alexander Sorkine-Hornung, and Luc Van Gool. The 2017 davis challenge on video object segmentation. *arXiv:1704.00675*, 2017. 20
- [55] Ekta Prashnani, Maneli Noorkami, Daniel Vaquero, and Pradeep Sen. A phase-based approach for animating images using video examples. In *CGF*, pages 303–311, 2017. 2
- [56] Alec Radford, Jong Wook Kim, Chris Hallacy, Aditya Ramesh, Gabriel Goh, Sandhini Agarwal, Girish Sastry, Amanda Askell, Pamela Mishkin, Jack Clark, et al. Learning transferable visual models from natural language supervision. In *ICML*, 2021. 3
- [57] Aditya Ramesh, Prafulla Dhariwal, Alex Nichol, Casey Chu, and Mark Chen. Hierarchical text-conditional image generation with clip latents. *arXiv preprint arXiv:2204.06125*, 2022. 2
- [58] Robin Rombach, Andreas Blattmann, Dominik Lorenz, Patrick Esser, and Björn Ommer. High-resolution image synthesis with latent diffusion models. In *CVPR*, 2022. 5
- [59] Chitwan Saharia, William Chan, Saurabh Saxena, Lala Li, Jay Whang, Emily L Denton, Kamyar Ghasemipour, Raphael Gontijo Lopes, Burcu Karagol Ayan, Tim Salimans, et al. Photorealistic text-to-image diffusion models with deep language understanding. *NeurIPS*, 2022. 2
- [60] Tamar Rott Shaham, Tali Dekel, and Tomer Michaeli. Singan: Learning a generative model from a single natural image. In *ICCV*, 2019. 2
- [61] Jing Shi, Wei Xiong, Zhe Lin, and Hyun Joon Jung. Instant-booth: Personalized text-to-image generation without test-time finetuning. *arXiv preprint arXiv:2304.03411*, 2023. 2, 3
- [62] Zhan Shi, Xu Zhou, Xipeng Qiu, and Xiaodan Zhu. Improving image captioning with better use of captions. *arXiv preprint arXiv:2006.11807*, 2020. 8
- [63] Aliaksandr Siarohin, Stéphane Lathuilière, Sergey Tulyakov, Elisa Ricci, and Nicu Sebe. Animating arbitrary objects via deep motion transfer. In *CVPR*, 2019. 2
- [64] Aliaksandr Siarohin, Stéphane Lathuilière, Sergey Tulyakov, Elisa Ricci, and Nicu Sebe. First order motion model for image animation. In *NeurIPS*, 2019.
- [65] Aliaksandr Siarohin, Oliver J Woodford, Jian Ren, Menglei Chai, and Sergey Tulyakov. Motion representations for articulated animation. In *CVPR*, 2021. 2

- [66] Uriel Singer, Adam Polyak, Thomas Hayes, Xi Yin, Jie An, Songyang Zhang, Qiyuan Hu, Harry Yang, Oron Ashual, Oran Gafni, et al. Make-a-video: Text-to-video generation without text-video data. In *ICLR*, 2023. 2
- [67] Jascha Sohl-Dickstein, Eric Weiss, Niru Maheswaranathan, and Surya Ganguli. Deep unsupervised learning using nonequilibrium thermodynamics. In *ICML*, 2015. 2
- [68] Jascha Sohl-Dickstein, Eric A. Weiss, Niru Maheswaranathan, and Surya Ganguli. Deep unsupervised learning using nonequilibrium thermodynamics. In *ICML*, 2015. 3
- [69] Jiaming Song, Chenlin Meng, and Stefano Ermon. Denoising diffusion implicit models. In *ICLR*, 2021. 5
- [70] Khurram Soomro, Amir Roshan Zamir, and Mubarak Shah. Ucf101: A dataset of 101 human actions classes from videos in the wild. *arXiv preprint arXiv:1212.0402*, 2012. 5, 13
- [71] Zineng Tang, Ziyi Yang, Chenguang Zhu, Michael Zeng, and Mohit Bansal. Any-to-any generation via composable diffusion. In *NeurIPS*, 2023. 2
- [72] Thomas Unterthiner, Sjoerd van Steenkiste, Karol Kurach, Raphaël Marinier, Marcin Michalski, and Sylvain Gelly. Fvd: A new metric for video generation. In *ICLR workshop*, 2019. 5, 13
- [73] Ruben Villegas, Mohammad Babaeizadeh, Pieter-Jan Kindermans, Hernan Moraldo, Han Zhang, Mohammad Taghi Saffar, Santiago Castro, Julius Kunze, and Dumitru Erhan. Phenaki: Variable length video generation from open domain textual description. In *ICLR*, 2023. 2
- [74] Vikram Voleti, Alexia Jolicoeur-Martineau, and Chris Pal. Mcvd-masked conditional video diffusion for prediction, generation, and interpolation. In *NeurIPS*, 2022. 2
- [75] Andrey Voynov, Qinghao Chu, Daniel Cohen-Or, and Kfir Aberman. $p+$: Extended textual conditioning in text-to-image generation. *arXiv preprint arXiv:2303.09522*, 2023. 4
- [76] Jiuniu Wang, Hangjie Yuan, Dayou Chen, Yingya Zhang, Xiang Wang, and Shiwei Zhang. Modelscope text-to-video technical report. *arXiv preprint arXiv:2308.06571*, 2023. 2
- [77] Xiang Wang, Hangjie Yuan, Shiwei Zhang, Dayou Chen, Jiuniu Wang, Yingya Zhang, Yujun Shen, Deli Zhao, and Jingren Zhou. Videocomposer: Compositional video synthesis with motion controllability. *arXiv preprint arXiv:2306.02018*, 2023. 1, 2, 5, 13
- [78] Yaohui Wang, Piotr Bilinski, Francois Bremond, and Antitz Dantcheva. Imaginator: Conditional spatio-temporal gan for video generation. In *WACV*, 2020. 2
- [79] Yaohui Wang, Di Yang, Francois Bremond, and Antitz Dantcheva. Latent image animator: Learning to animate images via latent space navigation. In *ICLR*, 2021. 2
- [80] Yaohui Wang, Xinyuan Chen, Xin Ma, Shangchen Zhou, Ziqi Huang, Yi Wang, Ceyuan Yang, Yinan He, Jiashuo Yu, Peiqing Yang, et al. Lavie: High-quality video generation with cascaded latent diffusion models. *arXiv preprint arXiv:2309.15103*, 2023. 2
- [81] Chung-Yi Weng, Brian Curless, and Ira Kemelmacher-Shlizerman. Photo wake-up: 3d character animation from a single photo. In *CVPR*, 2019. 2
- [82] Wenpeng Xiao, Wentao Liu, Yitong Wang, Bernard Ghanem, and Bing Li. Automatic animation of hair blowing in still portrait photos. In *ICCV*, 2023. 2
- [83] Jinbo Xing, Menghan Xia, Yuxin Liu, Yuechen Zhang, Yong Zhang, Yingqing He, Hanyuan Liu, Haoxin Chen, Xiaodong Cun, Xintao Wang, et al. Make-your-video: Customized video generation using textual and structural guidance. *arXiv preprint arXiv:2306.00943*, 2023. 2
- [84] Wei Xiong, Wenhan Luo, Lin Ma, Wei Liu, and Jiebo Luo. Learning to generate time-lapse videos using multi-stage dynamic generative adversarial networks. In *CVPR*, 2018. 2
- [85] Jun Xu, Tao Mei, Ting Yao, and Yong Rui. Msr-vtt: A large video description dataset for bridging video and language. In *CVPR*, 2016. 5, 13
- [86] Tianfan Xue, Jiajun Wu, Katherine Bouman, and Bill Freeman. Visual dynamics: Probabilistic future frame synthesis via cross convolutional networks. In *NeurIPS*, 2016. 2
- [87] Tianfan Xue, Jiajun Wu, Katherine L Bouman, and William T Freeman. Visual dynamics: Stochastic future generation via layered cross convolutional networks. *IEEE TPAMI*, 41(9):2236–2250, 2018. 2
- [88] Hu Ye, Jun Zhang, Sibo Liu, Xiao Han, and Wei Yang. Ip-adapter: Text compatible image prompt adapter for text-to-image diffusion models. *arXiv preprint arXiv:2308.06721*, 2023. 2, 3
- [89] Shengming Yin, Chenfei Wu, Jian Liang, Jie Shi, Houqiang Li, Gong Ming, and Nan Duan. Dragnuwa: Fine-grained control in video generation by integrating text, image, and trajectory. *arXiv preprint arXiv:2308.08089*, 2023. 2
- [90] Lijun Yu, Yong Cheng, Kihyuk Sohn, José Lezama, Han Zhang, Huiwen Chang, Alexander G Hauptmann, Ming-Hsuan Yang, Yuan Hao, Irfan Essa, et al. Magvit: Masked generative video transformer. In *CVPR*, 2023. 2
- [91] David Junhao Zhang, Jay Zhangjie Wu, Jia-Wei Liu, Rui Zhao, Lingmin Ran, Yuchao Gu, Difei Gao, and Mike Zheng Shou. Show-1: Marrying pixel and latent diffusion models for text-to-video generation. *arXiv preprint arXiv:2309.15818*, 2023. 2
- [92] Jiangning Zhang, Chao Xu, Liang Liu, Mengmeng Wang, Xia Wu, Yong Liu, and Yunliang Jiang. Dtvnet: Dynamic time-lapse video generation via single still image. In *ECCV*, 2020. 2
- [93] Lvmin Zhang, Anyi Rao, and Maneesh Agrawala. Adding conditional control to text-to-image diffusion models. In *ICCV*, 2023. 2
- [94] Yabo Zhang, Yuxiang Wei, Dongsheng Jiang, Xiaopeng Zhang, Wangmeng Zuo, and Qi Tian. Controlvideo: Training-free controllable text-to-video generation. *arXiv preprint arXiv:2305.13077*, 2023. 2
- [95] Yuechen Zhang, Jinbo Xing, Eric Lo, and Jiaya Jia. Real-world image variation by aligning diffusion inversion chain. *arXiv preprint arXiv:2305.18729*, 2023. 2
- [96] Jian Zhao and Hui Zhang. Thin-plate spline motion model for image animation. In *CVPR*, 2022. 2
- [97] Daquan Zhou, Weimin Wang, Hanshu Yan, Weiwei Lv, Yizhe Zhu, and Jiashi Feng. Magicvideo: Efficient video generation with latent diffusion models. *arXiv preprint arXiv:2211.11018*, 2022. 2, 5

DynamiCrafter: Animating Open-domain Images with Video Diffusion Priors

Supplementary Material

Contents

A Implementation Details	12
A.1 Network Architecture	12
A.2 Hyper-parameters	12
A.3 Training	12
B Additional Evaluation Details	13
B.1 Dataset and metric	13
B.2 Baselines	13
C User Study	13
D Details of Constructed Dataset	13
D.1 Dataset construction details	13
D.2 Statistics of the dataset	15
D.3 Human validation on the dataset	15
D.4 DynamiCrafter _{DCP}	15
E Other Controls	15
E.1 FPS Control	15
E.2 Multi-condition Classifier Free Guidance	15
F Limitations	17
G More Qualitative Results	20

Please check our project page <https://doubiu.github.io/projects/DynamiCrafter> for video results.

A. Implementation Details

A.1. Network Architecture

Our *DynamiCrafter* is built upon VideoCrafter, a latent VDM-based text-to-video (2TV) generation model, so we recommend that readers refer to VideoCrafter [8] for more details of the T2V backbone. It is worth noting that our approach of leveraging the video diffusion prior for image animation can theoretically be applied to any other T2V diffusion models that incorporate a cross-attention text-conditioning mechanism. To improve the reproducibility of our method, we provide a more detailed description of the network architecture for the FPS embedding layer and context query transformer. As depicted in Figure 11 (left), the FPS condition is embedded via Sinusoidal and several Fully-Connected (FC) layers activated by SiLU [25], which is then added to the timestep embedding f_{emb} . In Figure 11 (right), the context query transformer first projects the concatenation of frame-wise context queries and CLIP tokens

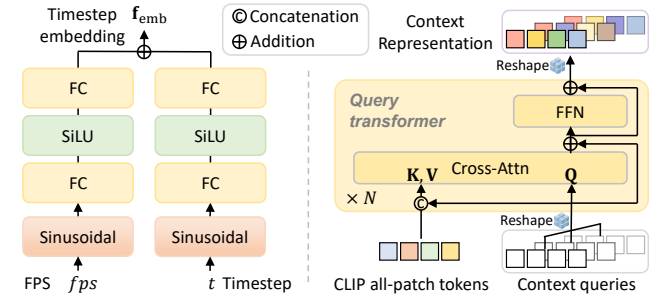


Figure 11. Network architecture of the FPS embedding layer (left) and query transformer for context representation learning (right).

into *keys* and *values*, while projecting context queries solely into *queries*. The cross-attention results are subsequently computed using the *keys*, *values*, and *queries*, and projected via a Feed-forward layer. The final frame-wise context representation is then employed through the spatial dual-attn transformer in the denoising U-Net, as illustrated in Figure 1 and Equation 2 in the main paper.

A.2. Hyper-parameters

Following [7], all architecture parameter details, diffusion process details, as well as training hyper-parameters are provided in Table 5, which should be mostly self-explanatory. Here we give some additional description for some parameters:

- Input channels (Architecture): The number of input tensor channels for the denoising U-Net, which is twice the channel number of \mathbf{z}_t due to the channel-wise concatenation of visual detail guidance.
- CA ctx sequence length (Dual-CA Conditioning): The token length of the context representations for each frame.

A.3. Training

Since we concatenate the conditional image latent with noisy latents in the channel dimension (*i.e.*, visual detail guidance in Section 3.2 of the main paper), we add additional input channels to the first convolutional layer. All available weights of the video diffusion model are initialized from the pre-trained checkpoints, and weights that operate on the newly added input channels are initialized to zero. We utilize only eight NVIDIA V100 GPUs to fine-tune the T2V model that is relatively resource-friendly in the context of developing an image-to-video diffusion model. As mentioned in Section 4.1 of the main paper, we fine-tune the T2V model using WebVid10M, primarily consists of real-world videos. Despite this, the model demon-

Table 4. Summary of open-domain (text-)image-to-video generation methods. *The resolution is obtained by inputting a square-sized image into these methods.

Method	Open-source	Verison (Date)	Resolution*	Duration	FPS	Text input	Description (visual condition injection)
VideoComposer	✓	23.06.29	256 × 256	2s	8	✓	The encoded image information is injected via frame-wise concatenation with the noisy latent.
I2VGen-XL	✓	23.10.30	256 × 448	3s	8	✗	Image information is injected by cross-attention via the global token from CLIP image encoder.
PikaLabs	✗	23.11.01	768 × 768	3s	24	✓	Unknown
Gen-2	✗	23.11.01	896 × 896	4s	24	✓	Unknown

strates strong generalizability when animating images that are even outside its domain, such as anime or paintings.

B. Additional Evaluation Details

B.1. Dataset and metric

To evaluate the quality and temporal coherence of synthesized videos in both the spatial and temporal domains, we report Fréchet Video Distance (FVD) [72] as well as Kernel Video Distance (KVD) [72], which evaluate video quality by measuring the feature-level similarity between synthesized and real videos based on the Fréchet distance and kernel methods, respectively. Specifically, they are computed by comparing 2048 model samples with samples from evaluation datasets, where we adopt commonly used UCF-101 [70] and MSR-VTT [85] for benchmarking. For UCF-101, we directly use UCF class names [7] as text conditioning, while for MSR-VTT, we utilize accompanied captions of each video from the dataset. We evaluate each error metric at the resolution of 256 × 256 with 16 frames.

B.2. Baselines

In the emerging field of open-domain image animation, there are limited baselines available for comparison. In this study, We evaluate our method against two open-source research works, *i.e.*, VideoComposer [77] and I2VGen-XL [12], and two proprietary commercial products, *i.e.*, PikaLabs [13] and Gen-2 [11], which are summarized in Table 4. Note that we employ the image-to-video (first-stage) generation of I2VGen-XL for the evaluation experiment, as its refinement stage (text-to-video) primarily functions as a super-resolution process, with the dynamics and temporal coherence already determined by the first stage.

C. User Study

The designed user study interface is shown in Figure 16. We collect 20 image cases with a wide range of content and styles from the Internet and create corresponding captions. We then generate the image animation results by either executing the official code [12, 77] or accessing the online demo interface [11, 13]. For the user study, we use these video results produced by shuffled methods based on the

same input still image (and text prompt, if applicable). In addition, we conceal the lower watermark region and standardize the all the produced results by first setting FPS=8, and then trimming the videos to two seconds at the same resolution level (256 × 448 for I2VGen-XL, while 256 × 256 for other methods). This process ensures a fair comparison by eliminating the potential impact of engineering tricks.

The user study is expected to be completed with 5–10 minutes (20 cases × 3 sub-questions × 5–10 seconds for each judgement). To remove the impact of random selection, we filter out those comparison results completed within three minutes. For each participant, the user study interface shows 20 video comparisons, and the participant is instructed to evaluate the videos for three times, *i.e* answering the following questions respectively: (i) “Which one has the best motion/dynamic quality?”; (ii) “Which one has the best temporal coherence?”; (iii) “Which results conform to the input image?”. Finally, we received 49 valid responses from the participants.

D. Details of Constructed Dataset

D.1. Dataset construction details

As depicted in Figure 8 of the main paper, we first filter out data with large camera movement, poor caption-video alignment, and Graphics/CGI content. We then feed captions to GPT4 [52] (temperature=0.2, frequency_penalty=0) to generate the following: *dynamic confidence*, which represents the level of confidence that the caption describes a dynamic scene, *dynamic wording*, such as “man doing push-ups”, and the category of this dynamic scene. The used dialog instructions are as follows:

User: You are an expert assistant. There some caption-video pairs in the dataset, and you can only access the captions. You need to check if the caption describes the scene dynamics in the video, for example some actions of humans and animals, etc. Please output the following: 1. Dynamic confidence. Output how confident you feel that it is describing a dynamic scene, from 0 to 100. 0 means lowest confidence and 100 means the highest confidence. 2. Dynamic wording. Output the subject followed by actions

Table 5. Hyperparameters for our *DynamiCrater*.

Hyperparameter	<i>DynamiCrater</i>
Spatial Layers	
<i>Architecture</i>	
LDM	✓
f	8
z -shape	$32 \times 32 \times 4$
Channels	320
Depth	2
Channel multiplier	1,2,4,4
Attention resolutions	64,32,16
Head channels	64
Input channels	8
Output channels	4
<i>Dual-CA Conditioning</i>	
Embedding dimension	1024
CA resolutions	64,32,16
CA txt sequence length	77
CA cxt sequence length	16
<i>FPS Conditioning</i>	
Embedding dimension	1280
FPS sampling range	5–30
<i>Concat Conditioning</i>	
Embedding dimension	4
Index of video frame	Random
Extension in temporal dim.	Repeat
Temporal Layers	
<i>Architecture</i>	
Transformer depth	1
Attention resolutions	64,32,16
Head channels	64
Positional encoding	✗
Temporal conv layer num	4
Temporal kernel size	3,1,1
Training	
Parameterization	ϵ
Learnable para.	Spatial layers \mathcal{P} with ctx CA
# train steps	100K
Learning rate	5×10^{-5}
Batch size per GPU	8
# GPUs	8
GPU-type	V100-32GB
Sequence length	16
Diffusion Setup	
Diffusion steps	1000
Noise schedule	Linear
β_0	0.00085
β_T	0.0120
Sampling Parameters	
Sampler	DDIM
Steps	50
η	1.0
Guidance scale s_{txt}	7.5
Guidance scale s_{img}	7.5

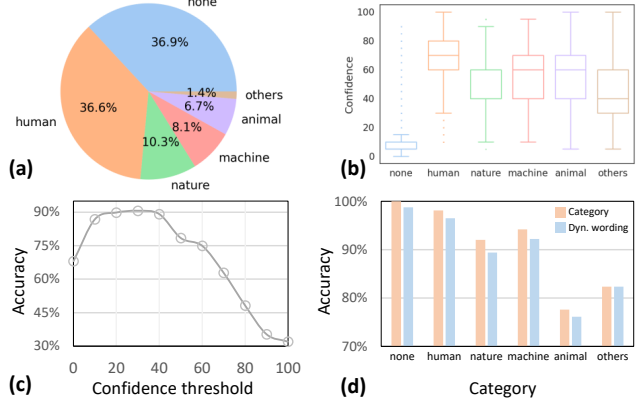


Figure 12. Statistics of the dataset and human validation results.

and corresponding objects, for example “man playing football”. It must be compact. Output “none” when the caption does not describe any scene dynamics. 3. Dynamic source category. Classify the dynamics, the categories are human, animal, nature, machine, others, and none. none is used when the corresponding dynamic wording is none. nature indicates those dynamics related to natural phenomena, while machine corresponds those movements related to vehicles and technical devices.

The input is in the format of “<question index>%<caption>”, The output must be in the format of “<question index>%<confidence>%<dynamic wording> %<dynamic source category>”. Here are some examples:

Input: [“1%%Woman in gym working out”, “2%%4k corporate shot of a business woman working on computer eating funny banana”, “3%%Rainy clouds sailing above a city”, “4%%View of the great salt lake”, “5%%Old house with a ghost in the forest at night or abandoned haunted horror house in fog.”]

Output: [“1%%80%%woman working out%%human”, “2%%80%%business woman working on computer, eating banana%%human”, “3%%50%%Rainy clouds sailing%%nature”, “4%%5%%none%%none”, “5%%10%%none%%none”].

Input captions are in an array: [caption1, caption2, ...].

System: Answer for every caption in the array and reply with an array of all completions.

Here are some sampled inputs and outputs (w/o index):

Input: [“Young man in bathrobe brushing his teeth in front of the window.”, “Summer green maple tree swinging in the wind.”, “Ripe rambutan fruits on a street market. sri lanka.”]

Output: [“70%%man brushing teeth%%human”, “50%%maple tree swinging%%nature”, “5%%none%%none”]

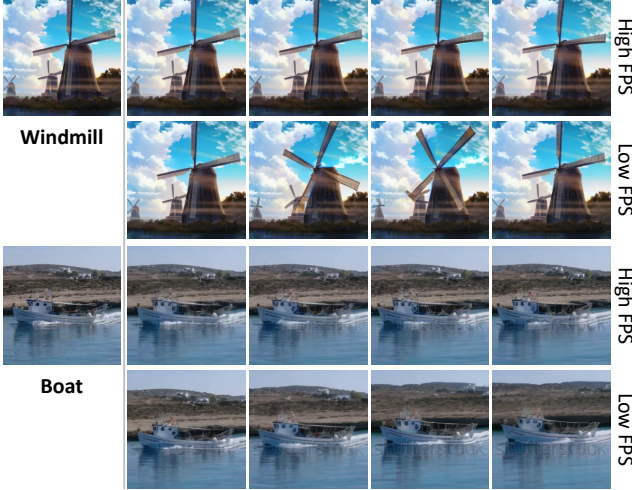


Figure 13. Visual comparisons of image animation results produced by our DynamiCrafter with FPS control.

D.2. Statistics of the dataset

The constructed dataset contains around 2.6 million caption-video pairs, with the corresponding statistics and dynamic confidence for each category shown in Figure 12 (a) and (b), respectively. We exclude certain combinations of classes, such as ‘animal&human’, ‘human&machine’, ‘animal&machine’ due to their small proportions. To support potential research on motions and dynamics, we will make the annotations of the constructed dataset publicly available.

D.3. Human validation on the dataset

We also validate GPT4’s responses through human judgement on randomly sampled 1K responses. We ask volunteers to determine if the original video caption describes a dynamic scene and if the dynamic wording and category generated by GPT4 are accurate. In Figure 12 (c), we plot an accuracy-threshold curve by adjusting the confidence threshold and calculating the accuracy based on human judgments of dynamic scenes. We observe that *dynamic confidence*=40 serves as a sweet spot in aligning with human judgement. The accuracy of dynamic wording and category for each category are shown in Figure 12 (d). The validation results indicate that GPT4’s responses generally align with human judgments, making them reliable for dataset annotation.

D.4. DynamiCrafter_{DCP}

Finally, we initialize DynamiCrater_{DCP} using an intermediate checkpoint (60K iterations) from DynamiCrafter, and then continue to train it with another 40K iterations using human category data in the constructed dataset with *dynamic wording* as text prompts. The baseline model is our



Figure 14. Visual comparisons of image animation results produced by various combinations of s_{img} and s_{txt} .

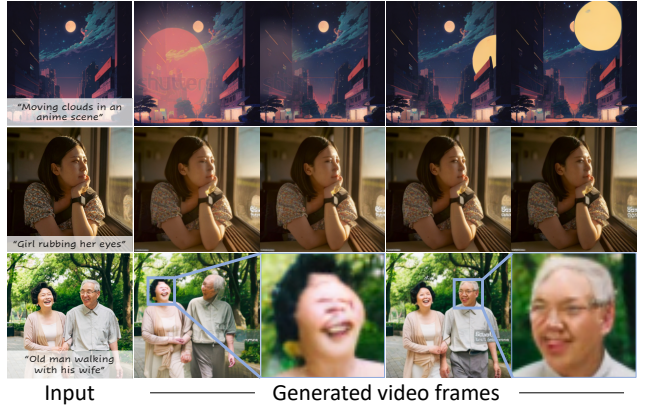


Figure 15. Failure cases of the challenging input condition in terms of semantic understanding (top), specific motion control with text (middle) and face distortion (bottom).

DynamiCrafter, trained for 100K iterations. In addition, we maintain all other settings identical for fair comparison. As mentioned in Section 5 of the main paper, we use CLIP-SIM to evaluate the performance of DynamiCrafter_{DCP}, considering that CLIP is an open-domain text-image representation learner and is capable of associating the dynamics in the image with the appropriate dynamic wording.

E. Other Controls

E.1. FPS Control

Since our model is also conditioned on FPS and trained with dynamic FPS, *i.e.* 5–30, it is capable of generating image animations with varying motion magnitudes, as demonstrated in Figure 13, where we show the results with ‘low FPS’ and ‘high FPS’ for simplicity.

E.2. Multi-condition Classifier Free Guidance

During inference, we adopt DDIM with multi-condition classifier guidance [27] and can adjust the introduced two guidance scales s_{img} and s_{txt} to trade off the impact of two

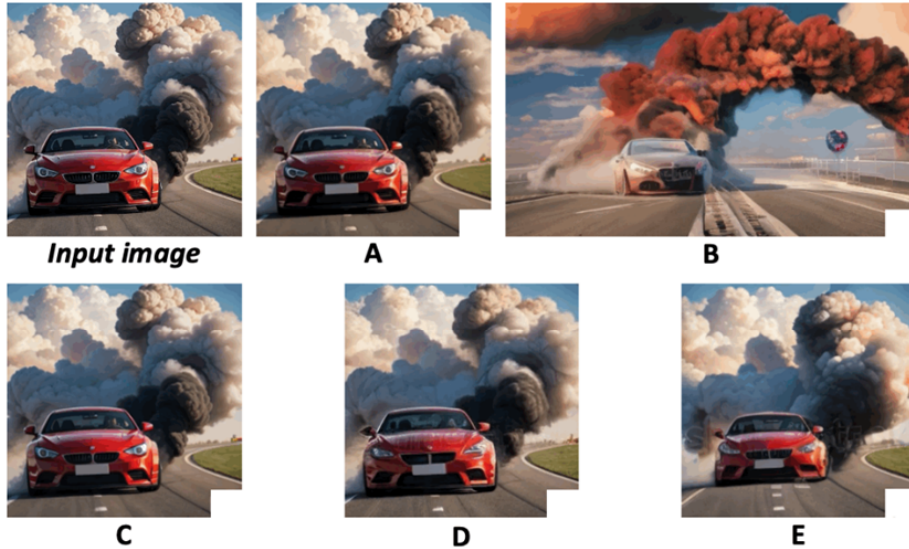
Instructions:

Please view the video results generated from the input images and text below. For each of the 20 comparison sets, there are 3 sub-questions (please separately choose the **best** one based on **motion/dynamic quality** and **temporal coherence** [single choice], and **select all** the results that **conform to the input image** [multiple choice]).

Note:

1. Good motion/dynamic quality means that the generated video should include certain motions/dynamics and be natural, consistent with the image context and the text's control of dynamics (if any).
2. Good content temporal coherence refers to coherent visual content without unnatural sudden changes or distortions.
3. Conforming to the input image means that the video content's details (objects, textures, color tones, etc.) consistently match the input image, with only differences in dynamics.
4. Please ignore the impact of the missing corner in the bottom right of the results.

"car driving down a road with smoke coming out of it"



1.1 Which one has the best motion/dynamic quality?

- A B
 C D
 E

1.2 Which one has the best temporal coherence?

- A B
 C D
 E

1.3 Which results conform to the input image?

- A B
 C D
 E

Figure 16. Designed user study interface. Each participant is required to evaluate 20 video comparisons and respond to three corresponding sub-questions for each comparison. Only one video is shown here due to the page limit.

control signals, as mentioned in Section 4.1 of the main paper. Specifically, it will affect how strongly the generated samples correspond with the input image and how strongly

they correspond with the text prompt. Here we present the visual comparisons in Figure 14. In most cases, setting $s_{\text{img}} = s_{\text{txt}} = 7.5$ works well, as the generated ani-

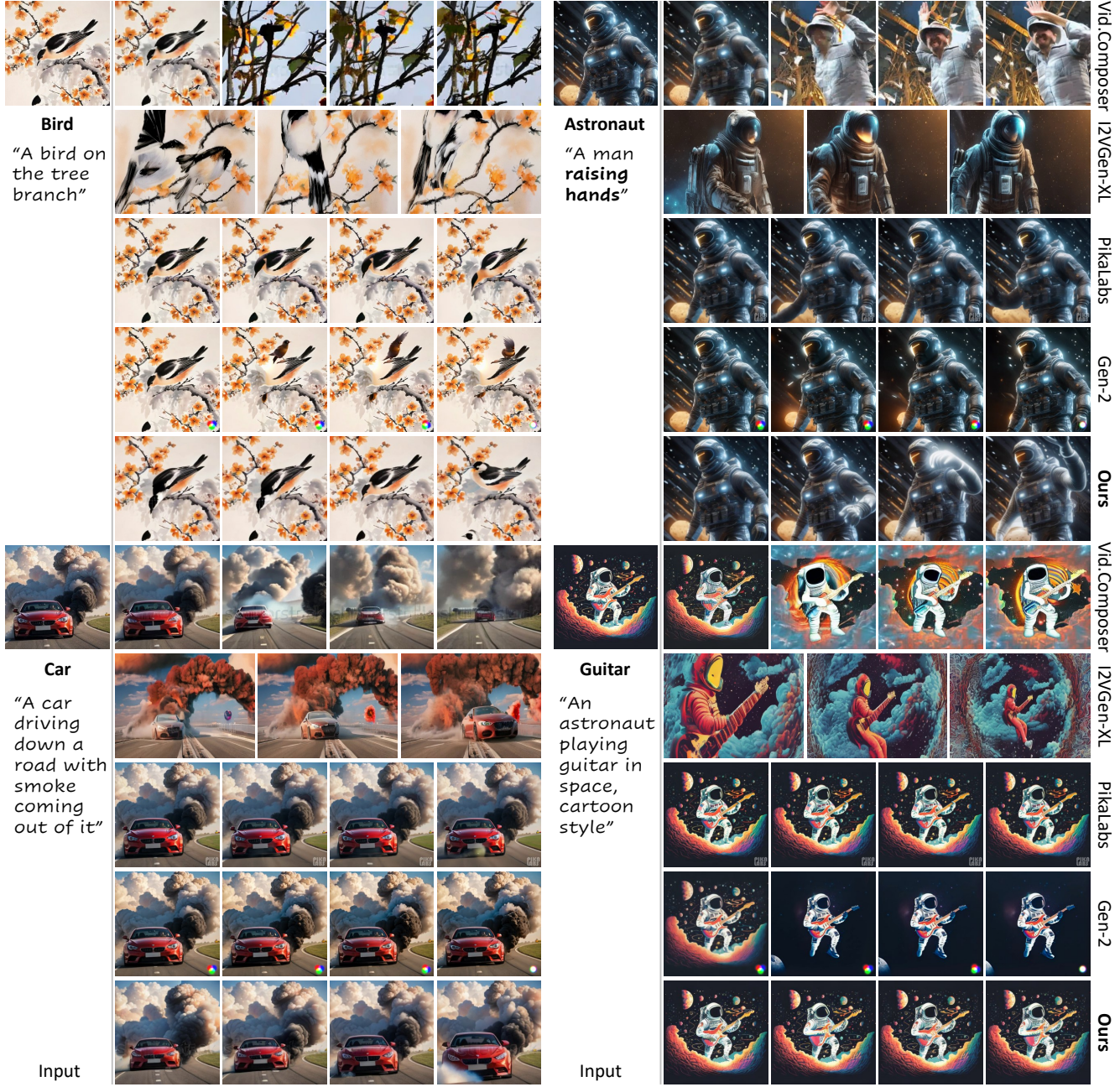


Figure 17. Visual comparisons of image animation results from VideoComposer, I2VGen-XL, PikaLabs, Gen-2, and our *DynamiCrafter*.

mations can well adhere to the input image and reflect the text prompt, as shown in Figure 14(top). By decreasing s_{txt} , the animation results tend to ignore the text condition, e.g., “dancing”, as shown in Figure 14(middle). Conversely, if s_{img} is reduced, the results may not conform to the input image but well reflect the text prompt (see Figure 14(bottom)). This multi-condition classifier guidance offers greater flexibility based on user requirements.

F. Limitations

Our approach is limited in several ways. Firstly, if the input image condition cannot be semantically understood, our model might struggle to produce convincing videos. Secondly, although we construct a dataset to improve motion control with text, which still lacks precise motion descriptions, rendering the inability to generate specific motions. Additionally, we adopt the LatentVDM pre-trained at low resolutions and with short durations due to limited comput-

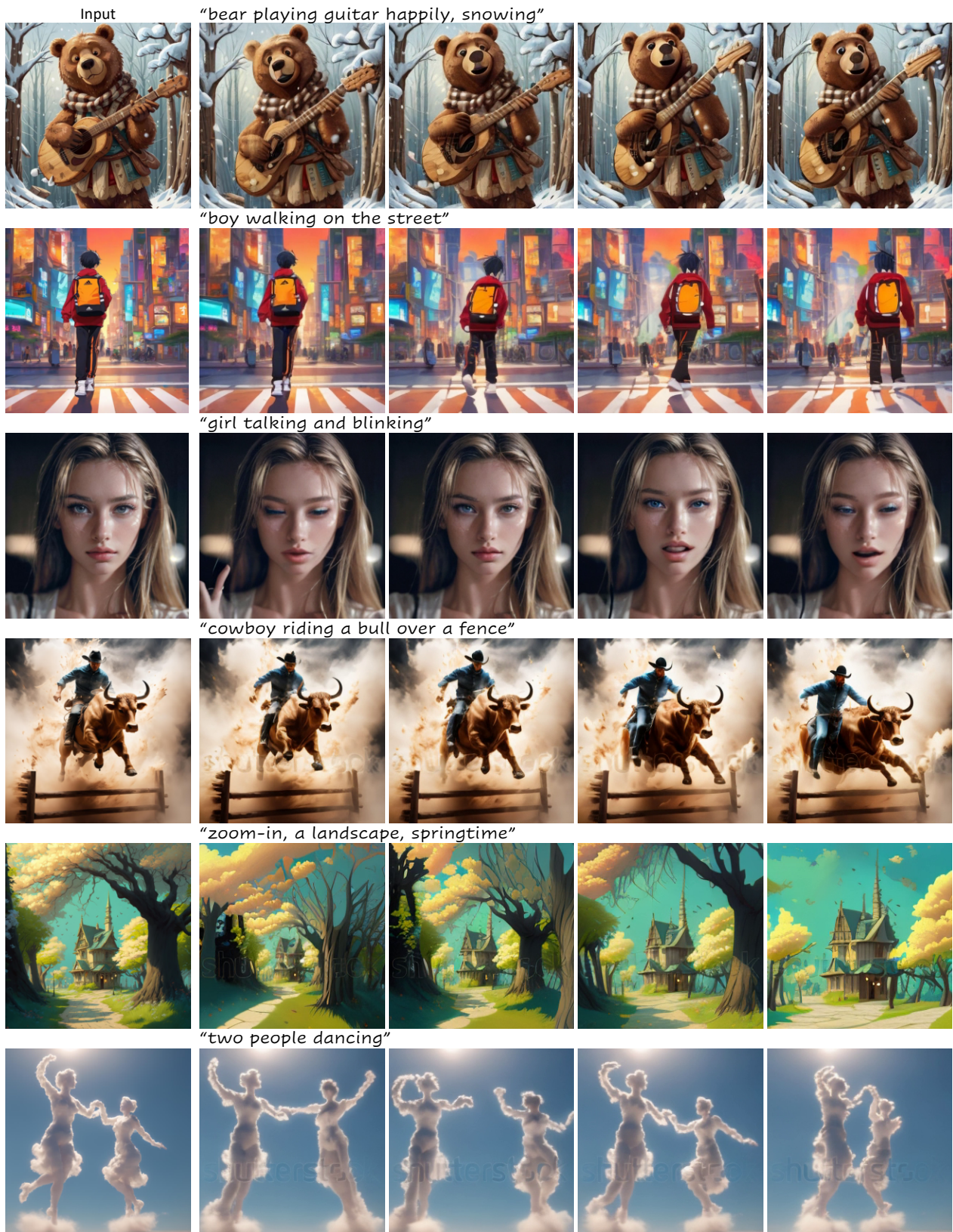


Figure 18. Gallery of our image animation results.

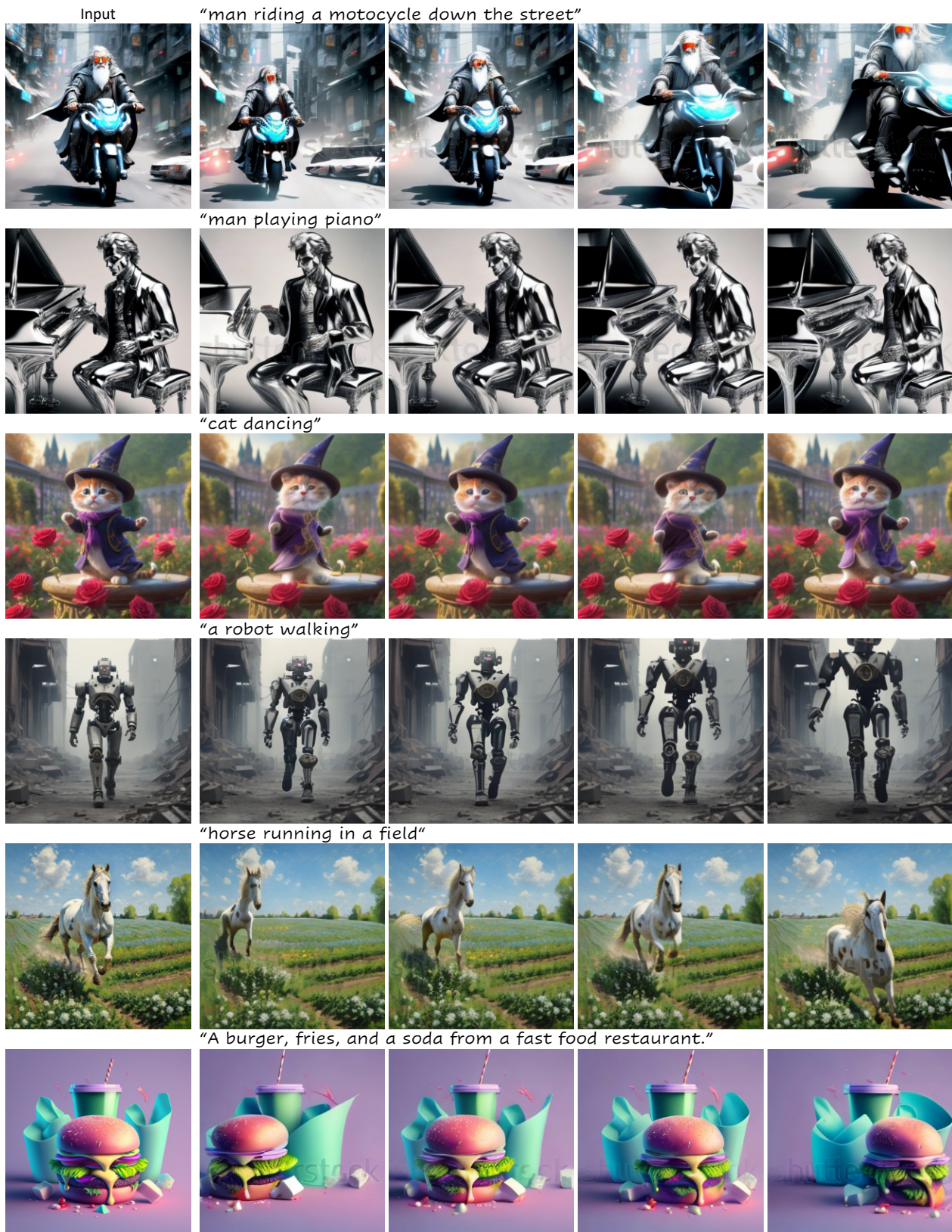


Figure 19. Gallery of our image animation results.

tational resources, resulting in inheriting its slight flickering artifacts in high-frequency regions (see supplemental video results) and human face distortion issues, which are technically caused by the frame-wise VAE decoding. Thus the resultant frame quality of our method (such as resolution and fidelity) and video length may limit practical applications. Consequently, our method may not be ready for product (in contrast to commercial products like PikaLabs and Gen-2). Figure 15 shows the examples of the mentioned failure cases. We leave these directions as future works.

G. More Qualitative Results

More qualitative comparisons. In addition to Figure 4 in the main paper, we provide more qualitative comparisons in Figure 17. Consistent with the observations in the main paper, VideoComposer struggles to produce coherence video frames and tends to be misled by the text prompt. I2VGen-XL fails to preserve the local visual details of the input image and can only generate animations that semantically resemble the input. PikaLabs tends to generate still videos or videos with limited dynamics. Gen-2 may incorrectly interpret the given image, rendering unreasonable results and temporal inconsistency (as seen in the ‘Bird’ and ‘Guitar’ cases). Moreover, these baseline methods have difficulty considering the text prompt for motion control (*e.g.*, *raising hands* in the ‘Astronaut’ case). In contrast, our approach can produce image animations with natural dynamics, better adherence to the input image, and motion control guided by the text prompt.

Gallery of our results. We show more image animation results produced by our method in Figure 18 and Figure 19. We collect those input images from the Internet, DAVIS [54], and JourneyDB [53].

Video results. We provide the video result at <https://doubiiu.github.io/projects/DynamiCrafter>. It contains the following parts: i). Showcases produced by our method, ii). Comparisons with baseline methods, iii). Motion control using text, iv). Applications, v). Other controls, vi). Ablation study, and vii). Limitations.